Published in final edited form as:

Prostate. 2021 July ; 81(10): 618–628. doi:10.1002/pros.24136.

The influence of low-carbohydrate diets on the metabolic response to androgen-deprivation therapy in prostate cancer

Jen-Tsan Chi, M.D. Ph.D[1,*], **Pao-Hwa Lin, Ph.D.**[2], **Vladimir Tolstikov, Ph.D.**[3], **Taofik Oyekunle, M.S.**[4], **Gloria Cecilia Galván Alvarado, Ph.D.**[5], **Adela Ramirez-Torres, Ph.D.**[5], **Emily Y. Chen, B.S.**[3], **Valerie Bussberg, B.S.**[3], **Bo Chi**[1], **Bennett Greenwood, M.S.**[3], **Rangaprasad Sarangarajan, B Pharm, Ph.D.**[3], **Niven R. Narain, Ph.D.**[3], **Michael A. Kiebish, Ph.D.**[3], **Stephen J. Freedland, M.D.**[5,6,*]

[1]Department of Molecular Genetics and Microbiology, Center for Genomics and Computational Biology

[2]Department of Medicine, Division of Nephrology, Duke University Medical Center, Durham, North Carolina USA

[3]BERG, Framingham, MA USA

[4]Duke Cancer Institute, Duke University Medical Center, Durham, NC USA

[5]Center for Integrated Research in Cancer and Lifestyle, Cedars-Sinai, Los Angeles, CA

[6]Durham VA Medical Center, Durham, NC, USA

Abstract

Prostate cancer (PC) is the second most lethal cancer for men. For metastatic PC, standard first line treatment is androgen deprivation therapy (ADT). While effective, ADT has many metabolic side effects. Previously, we found in serum metabolome analysis that ADT reduced androsterone sulfate, 3-hydroxybutyric acid, acyl-carnitines but increased serum glucose. Since ADT reduced ketogenesis, we speculate that low-carbohydrate diets (LCD) may reverse many ADT-induced metabolic abnormalities in animals and humans. In a multi-center trial of PC patients initiating ADT randomized to no diet change (control) or LCD, we previously showed that LCD intervention led to significant weight loss, reduced fat mass, improved insulin resistance and lipid profiles. To determine whether and how LCD affects ADT-induced metabolic changes, we analyzed serum metabolites after 3-, and 6-months of ADT on LCD vs. control. We found androsterone sulfate was most consistently reduced by ADT and was slightly further reduced in

[*]Corresponding Authors: Jen-Tsan Chi: jentsan.chi@duke.edu, 1-919-6684759, 101 Science Drive, DUMC 3382, CIEMAS 2177A, Durham, NC 27708, Stephen J. Freedland: stephen.freedland@cshs.org, 1-310-423-3497, 8635, W. Third St., Suite 1070W, Los Angeles, CA 90048.

Author contributions statement: JTC: data analysis, manuscript writing – original draft, review and editing. PHL: Conceptualization, data analysis, manuscript writing. VT, VB, NRN, BG, RS: methodology, data acquisition, statistical analysis. TO: statistical analysis. EC: methodology, project, administration, data acquisition, statistical analysis. BC: data analysis, CGA and AR: manuscript writing. MAK: Conceptualization, methodology, project administration, data acquisition, statistical analysis. SJF: Conceptualization, funding acquisitions, manuscript writing.

Conflict of interest statement: No conflict of Interest.

Data Availability Statement:
The metabolomic data will be made available to the academic community upon publication of the manuscript.

the LCD arm. Contrastingly, LCD intervention increased 3-hydroxybutyric acid and various acyl-carnitines, counteracting their reduction during ADT. LCD also reversed the ADT-reduced lactic acid, alanine and S-adenosyl Methionine (SAM), elevating glycolysis metabolites and alanine. While the degree of androsterone reduction by ADT was strongly correlated with glucose and indole-3-carboxaldehyde, LCD disrupted such correlations. Together, LCD intervention significantly reversed many ADT-induced metabolic changes while slightly enhancing androgen reduction. Future research is needed to confirm these findings and determine whether LCD can mitigate ADT-linked comorbidities and possibly delaying disease progression by further lowering androgens.

Keywords

ADT; Prostate Cancer; low carbohydrate diet; ketogenesis; metabolomics; androgen sulfate; 3-hydroxybutyric acid; 3-formyl indole; indole-3-carboxaldehyde

Introduction

Prostate cancer (PC) is the most common non-skin cancer and the second leading cause of cancer mortality for men in the US [1]. In 2020, 191,930 new cases of PC and 33,330 deaths from PC were estimated [2]. For men with non-metastatic disease who require treatment, local therapy is not always curative. While systemic therapies, such as chemotherapy and novel hormonal agents, that improve overall survival in late-stage PC [3,4] are being used in earlier stages, these therapies can have significant side effects including elevated risk for cardiovascular diseases [5]. Moreover, the backbone of systemic treatment for PC remains androgen deprivation therapy (ADT) by decreasing male hormone levels to reduce tumor growth.

In a typical Western diet, usually 40–60% kcals come from carbohydrates, whereas low-carbohydrate diets (LCDs) usually include <20% carbohydrate kcals [6]. LCDs and ketogenic diets (a form of a very low carbohydrate diet) improve diabetes and aid with weight loss [7–9]. Since the common side effects of ADT include weight gain, body fat gain, increased adiposity and insulin resistance, LCDs may benefit PC patients by minimizing the side effects during this therapy. Thus, the main objective of the CAPS1 (Carbohydrate and Prostate Study 1) study was to compare the impact of a 6-month LCD intervention vs. a control arm on insulin resistance in PC patients initiating ADT. Results from the comparison between the two arms[10] showed that at 3-month of intervention, LCD group significantly reduced weight, improved insulin resistance, hemoglobin A1c, high-density lipoprotein (HDL), and triglyceride levels. However, at 6-month, only weight loss and HDL remained significantly different between arms, though insulin resistance when measured throughout the study was significantly improved. We also observed other markers that reversed toward baseline at 6-month, though we were limited in power to detect significant associations due to our small sample (n=29). Given the multiple potential benefits seen, the LCD deserves further examination.

Metabolomic analysis allow an integrated read-out of all the upstream biochemical pathways associated with various oncogenic genetic drivers, therapeutic intervention and lifestyle

choices [11,12]. Thus, metabolomic results can provide insights into various factors during tumor progression, invasion and metastasis [13]. For example, the metabolomic analysis of prostate tumors identified the relevant role sarcosine-related pathways in PC oncogenesis [14,15]. Other analyses aimed to identify therapeutic targets to treat PC[16–18] or elucidate the metabolic response to the PC treatments. While ADT is the standard treatment for metastatic PC, it results in significant metabolic side effects. To date, only three studies have analyzed the serum metabolome from PC patients receiving ADT [19–21]. Briefly, Saylor et al. reported 56 significantly altered metabolites after receiving 3 months of ADT, including androgen steroids, bile acid metabolites and lipid β- and Ω-oxidation [20]. The second study identified seven ADT-associated metabolites, which reverted to control levels after ADT was stopped [19]. Recently, we reported the serum metabolomic and lipidomic profiling of PC patients in the control arm of the CAPS1 trial after 3 and 6 months of ADT treatment [21]. As expected, ADT lowered androsterone sulfate and the degree of reduction was significantly correlated with increased serum glucose, supporting a diabetogenic role of ADT. ADT also reduced 3-hydroxybutyric acid, many acyl-carnitines and indole-3-carboxaldehyde, a tryptophan-derived metabolite of the gut microbiome that serves as an agonist for the aryl hydrocarbon receptor to regulate mucosal immunity [22]. Given the metabolic benefits observed in patients in the LCD arm of the CAPS1 study [10], the main purpose of this study was to apply serum metabolomic technology to evaluate the metabolic impact of the LCD intervention on the metabolic effects in response to ADT. In addition, we evaluated how LCD may affect the efficacy of ADT as measured by reduction of serum androgens and thereby provide potential therapeutic benefits.

Participants and Methods

Study Design

As previously described [1021], IRB approval was obtained at Duke, Durham Veterans Affairs Medical Center [VAMC], and Greater Los Angeles VAMC for the CAPS1 trial. PC men initiating ADT were approached and if they agreed to participate, they signed a written consent that allowed future analyses. Clinical data and fasting serum samples were collected at baseline prior to ADT (BL) and three (M3) and six months (M6) post-randomization and post initiation of ADT. Key eligibility included men about to begin hormonal therapy (LHRH agonist, LHRH-antagonist, or orchiectomy) for PC with an anticipated duration of ≥6 months, BMI ≥24 kg/m^2, and phone access to speak with the dietitian. Key exclusion criteria included medication-controlled diabetes, taking any medications that may interfere with insulin metabolism, already consuming an LCD, being vegetarian/vegan, or baseline screening HbA1c >7%. A total of 40 eligible participants were randomized immediately after the baseline assessment and received the intervention assignment. A total of 29 participants completed the 6-month visit and had complete data including blood specimen and their data were used for this report (N=11 LCD, N=18 control). Participants in the control arm received standard care and were asked to make no changes in diet or exercise pattern. Those in the LCD arm received individual coaching from the study dietitian to reduce carbohydrate intake to ≤20 gram/day and to walk for ≥30 minutes/day for 5 days/week. The study dietitian talked to the participants weekly for 3 months then bi-weekly for another 3 months. In this manuscript, we report the results of how LCD affected serum

metabolomics as compared to the control arm as the metabolic changes from ADT alone from CAPS1 have been previously described[21].

Data Collection and analysis

At each visit, weight (without shoes and in light clothing) and height were measured, and fasting blood was collected for blood chemistry. Fasting blood was analyzed for PSA, insulin, glucose, lipids, and high sensitivity C-reactive protein (hsCRP). PSA, glucose and lipids were measured by commercial laboratories (LabCorp for Duke and Durham VAMC sites and Greater LA VAMC clinical lab for the LA site). Insulin was measured in batch at study completion using banked serum, which had been stored at −80°C, using an electro-chemiluminescent immunoassay using an SI-2400 imager and assay kits from Meso Scale Discovery (Rockville, MD) by Duke Immunoassay Laboratory. Insulin resistance, as estimated by the homeostatic model assessment (HOMA), was calculated using the approximation (glucose*insulin)/22.5.

Fasting blood samples collected at BL, M3, and M6 were used for metabolomics analysis utilizing GC/MS-TOF (Gas chromatography–Mass Spectrometry Time of Flight analyzer), QqQ LC (Liquid Chromatography)-HILIC (Hydrophilic interaction chromatography)-MS/MS, and TripleTOF LC-RP-MS as described previously [21,23].

Metabolomics Analysis

Serum samples for metabolomics analysis were prepared as previously described[21,24–27]. Metabolite extraction was achieved using a mixture of isopropanol, acetonitrile, and water at a ratio of 3:3:2 v/v. Extracts were divided into three parts: 75 uL for gas chromatography combined with time-of-flight high-resolution mass spectrometry, 150 uL for reversed-phase liquid chromatography coupled with high-resolution mass spectrometry, and 150 uL for hydrophilic interaction chromatography with liquid chromatography and tandem mass-spectrometry, and analyzed as previously described[21,24–27]. We used the NEXERA XR UPLC system (Shimadzu, Columbia, MD, USA), coupled with the Triple Quad 5500 System (AB Sciex, Framingham, MA, USA) to perform hydrophilic interaction liquid chromatography analysis, NEXERA XR UPLC system (Shimadzu, Columbia, MD, USA), coupled with the Triple TOF 6500 System (AB Sciex, Framingham, MA, USA) to perform reversed-phase liquid chromatography analysis, and Agilent 7890B gas chromatograph (Agilent, Palo Alto, CA, USA) interfaced to a Time-of-Flight Pegasus HT Mass Spectrometer (Leco, St. Joseph, MI, USA). The GC system was fitted with a Gerstel temperature-programmed injector, cooled injection system (model CIS 4). An automated liner exchange (ALEX) (Gerstel, Muhlheim an der Ruhr, Germany) was used to eliminate cross-contamination from the sample matrix that may occur between sample runs. Quality control was performed using metabolite standards mixture and pooled samples applying methodology preciously described [24,27]. A quality control sample containing a standard mixture of amino and organic acids purchased from Sigma-Aldrich as certified reference material, was injected daily to perform analytical system suitability test and monitor recorded signals for day to day reproducibility as previously described [25,26]. A pooled quality control sample was obtained by taking an aliquot of the same volume of all samples from the study and injected daily with a batch of analyzed samples to determine the optimal

dilution of the batch samples and validate metabolite identification and peak integration. Collected raw data was manually inspected, merged, imputed and normalized to calculate the changes of metabolites in all the specimen. Metabolite identification was performed using in house authentic standards analysis. Metabolite annotation was used utilizing recorded retention time and retention indexes, recorded MSn and HRAMSn data matching with METLIN, NIST MS, Wiley Registry of Mass Spectral Data, HMDB, MassBank of North America, MassBank Europe, Golm Metabolome Database, SCIEX Accurate Mass Metabolite Spectral Library, MzCloud, and IDEOM databases.

Metabolite pathway analysis

Metabolomic data were analyzed as previously described by Tolstikov et al.[26]. Identified metabolites were subjected to pathway analysis with MetaboAnalyst 4.0, using Metabolite Set Enrichment Analysis (MSEA) module which consists of an enrichment analysis relying on measured levels of metabolites and pathway topology and provides visualization of the identified metabolic pathways. Accession numbers of detected metabolites (HMDB, PubChem, and KEGG Identifiers) were generated, manually inspected, and utilized to map the canonical pathways. MSEA was used to interrogate functional relation, which describes the correlation between compound concentration profiles and clinical outcomes.

Statistical Analysis

Significant changes were examined by ANOVA and shown in heatmaps and box plots. Impacted metabolic pathways were selected and mapped by using MetaboAnalyst 4.0 (https://www.metaboanalyst.ca/) [28]. Pearson correlation was conducted to examine associations between clinical variables and metabolites. Volcano plots were used to visually examine the changes in metabolites at M3 and M6 from baseline. The changes of metabolites at M3 and M6 were normalized against the BL using the attached Python scripts (supplemental file 1) modified from previous studies of transcriptional response[29–32] to derive the ADT-induced changes of all metabolites at M3 and M6 from corresponding BL in the control and LCD arms. Given the small number of men included in the study, no formal power calculations were done and all results are considered hypothesis-generating.

Results

Serum metabolites and metabolic pathways altered after 3 and 6 months of ADT in the LCD arm

As previously reported[10], participants in the control and LCD arms were similar in age (66 (SD)), weight (BMI of 29.0 (SD)), race composition, baseline dietary intakes and PSA levels (CAPS1 main result). We measured and identified metabolites that were altered in the LCD arm between BL (immediately before ADT) and after 3 (M3) and 6 months (M6) of ADT. Among the 439 metabolites identified in serum samples (methods of detection and validation in the methods), 32 metabolites were identified showing at least a 1.2-fold change and t-tests $p<0.05$ at M3 relative to BL. The top metabolites at M3, as shown in volcano plots (Fig 1A, Supplemental Table 1), included an increase in 3-hydroxybutyric acid, 2 hydroxy-butyric-carnitine. Also, there was a reduction in the androsterone sulfate and allantoin. As several selected metabolites belong to similar metabolic pathways, we

employed Metabolite Set Enrichment Analysis (MSEA)[33] to evaluate the potential enrichment of functionally related metabolites covering various metabolic pathways. The top MSEA-identified altered pathways at M3 included alanine metabolism, citric acid cycle, estrone metabolism, carnitine synthesis, gluconeogenesis, androgen/estrogen metabolism and glycolysis (Fig 1B).

Using similar approaches, 25 metabolites were identified between M6 vs. BL as having at least 1.2-fold change and t-tests $p<0.05$ and shown in volcano plots (Fig 1C, Supplemental Table 2). At M6, the top changes included the reduction in androsterone sulfate, malonyl-carnitine and 2-keosiovalerate. Several carnitines were also found to be increased, such as hydroxyproline and tiglycarintine. The top altered pathways at M6 identified by MSEA included catecholamine biosynthesis, methyl histidine metabolism, androgen/estrogen metabolism, estrone metabolism and carnitine metabolism (Fig 1D).

ADT-induced metabolic changes in both control and LCD arms

To identify metabolites whose changes were statistically significant in each arm, we applied ANOVA - Simultaneous Component Analysis (ASCA module, MetaboAnlyst 4.0) to uncover the major patterns associated with the time points and the treatments. We found that androsterone sulfate was reduced by ADT in both control and LCD arms (Fig 2A). This suggests that LCD did not affect the ADT-reduced androsterone sulfate. Instead, the degree of androsterone sulfate reduction (Fig 2B), despite not being statistically significant (M3: $p=0.07$, M6: $p=0.08$), tended to be *greater* in the LCD arm than the control arm. Next, we calculated the changes of metabolites before and after ADT in each participant in both control and LCD arms (Supplemental Fig 1A). These changes were then arranged by hierarchical clustering and the resultant heatmap shows the individual variations in the metabolic changes of individual participants (Supplemental Fig 1A). In the heatmap (Fig 2C) showing the ADT-induced metabolic changes from BL, we noted that the reduced androsterone sulfate was co-clustered with similar reduction of other androgens, including DHEA sulfate and pregnenolone sulfate. The ADT-reduced DHEA and pregnenolone sulfate also trended lower in the LCD arm, without reaching statistical significance. Overall, this finding suggests the potential of LCD to potentially and slightly enhance the ADT-induced reduction in androgens.

ADT-induced metabolic changes reversed by LCD

In the control arm, 3-hydroxybutyric acid was reduced at both M3 and M6 (Fig 3A) [21]. However, it was significantly increased at M3 in the LCD arm, and though the increase was somewhat mitigated at M6, it remained higher than BL (Fig 3A). The heatmap showing individual level data also showed that 3-hydroxybutyric acid was reduced in the control arm (blue) and increased in the LCD arm (yellow) (Fig 3B). In the heatmap, 3-hydroxybutyric acid was in a cluster of metabolites which were repressed in the control arm but elevated in the LCD arm (Supplemental Fig 1A, red bar expanded into Supplemental Fig 1C). Other than 3-hydroxyburtyric acid, these co-clustered metabolites included 2-hydroxybutyric acid, 3-hydroxy-3-methyl-glutaryl-carnitine and 3-aminobutyrate. Similarly, while many acyl-carnitines were noted to be reduced by ADT in the control arm [21], in the LCD arm, many acyl-carnitines, including hydroxy-butyryl-carnitine, tiglyl-carnitine, pimelyl-carnitine, 3-

hydroxyoctanoyl-carnitine, decanoyl-carnitine, 6-ketodecanoyl-carnitine, dodecanoyl-carnitine, dodecenoyl-carnitine, decanoyl-carnitine, decenoyl-carnitine were increased (Fig 3B). Therefore, the changes of these acyl-carnitines may be tightly associated with the ketone-related metabolites, indicating their potential metabolic connection. These results indicate that LCD reversed the ADT-reduced ketones and acyl-carnitines levels (Supplemental Fig 1C) and linking these two classes of metabolites found to be reduced by ADT[21]. Importantly, LCD reversed the reduction of these ketone metabolites and acyl-carnitines, one of the most prominent metabolic effects of ADT. Therefore, some of the ADT-induced changes seen in the control arm persisted in the LCD arm (such as reduced androgens) while others (such as reduced ketones and acyl-carnitines) were mitigated/reversed in the LCD.

Other ADT-induced metabolites were reversed in the LCD arm

While baseline levels of lactic acid were similar between control and LCD arms, it was slightly increased by ADT in the control arm but reduced in the LCD arm (Fig 4A). Indeed, the levels of lactic acids were significantly higher in the control vs. LCD arm at both M3 ($p<0.0001$) and M6 ($p=0.0004$) (Fig 4A). As shown in the heatmap (Fig 4B), the ADT-induced changes in lactic acid co-clustered with pyruvate, another metabolite in the glycolysis pathway, potentially reflecting decreased glycolysis in the LCD arm. Similar relationship has been described in the transcriptional analysis[34,35].

Similar trend was also observed for alanine, which remained relatively unchanged by ADT in the control arm, but decreased in the LCD arm so that the levels were significantly lower in the LCD arm at both M3 ($p=0.0001$) and M6 ($p=0.0053$) relative to corresponding time points in the control arm (Fig 4C). Such an opposite pattern between the control and LCD arms was also found for other co-clustered amino acids, including the branched-chain amino acids (valine, isoleucine and leucine) and tyrosine, lysine, leucine, isoleucine, cytosine, methionine, asparagine, histidine, proline, glutamine, arginine and tryptophan and its metabolite kynurenine (Fig 4D)[36].

Similarly, SAM (S-adenosyl-L-methionine) was slightly increased in the control arm and slightly reduced in the LCD arm such that the levels at M6 were significantly different between arms (Fig 4E, $p=0.0034$). Such a pattern of SAM was found to be co-clustered with several other sulfur-containing amino acids, including S-adenosyl-L-methioninamine, cysteine and cystine (Fig 4F). Similar pattern of changes in control and LCD arm was also observed in other amino acids (Fig 4D). Similarly, succinyl-adenosine, a metabolite accumulated in patients with Adenylosuccinate Lyase deficiency[37], was increased by ADT in the control group (Supplemental Fig 2). However, LCD abolished the ADT-induced increase in succinyl-adenosine.

Correlation of blood chemistry with the ADT-induced changes in androsterone sulfate

Although all androgens were expected to be reduced by ADT in both arms, androsterone sulfate was the most consistently reduced metabolite at both time points in both arms (Fig 1A, C). However, there were still individual heterogeneity in the degree of androgen suppression. Therefore, we reasoned that ADT-reduced androsterone sulfate may provide a

quantitative assessment of ADT efficacy to quantify the correlation with different blood chemistry and serum metabolites. First, we calculated the correlation between various blood chemistry measures and androsterone sulfate. In the control arm, the ADT-induced decreased androsterone sulfate was negatively correlated with glucose levels at both M3 ($p<0.001$, $r=-0.811$) and M6 ($p=0.0021$, $r=-0.660$) (Fig 5A, B). This indicates that a stronger reduction of androsterone sulfate was associated with increased glucose levels, supporting the diabetogenic tendency of the ADT. In contrast to glucose, the changes in androsterone sulfate were not significantly correlated with total cholesterol, LDL or insulin in either control or LCD arm (Supplemental figure 3A–C). Importantly, these correlations between glucose and androsterone sulfate disappeared in the LCD arm, suggesting that LCD disrupted the tight correlation between ADT response and increased serum glucose (Fig 5A, B).

Identify serum metabolites whose changes correlate with androsterone sulfate

Next, we calculated the ADT-induced changes in serum metabolome that correlated with the ADT-affected androsterone sulfate in both arms (Supplemental Table 3). LCD altered many observed correlations in the control arm at M3, but this was partially restored at M6. For example, there is a strong correlation between androsterone sulfate and other androgens, including pregnenolone sulfate and DHEA-androsterone in the control arm at both M3 and M6 (Supplemental Table 3) [21]. While such correlation still existed between pregnenolone and androsterone (Supplemental figure 3A), LCD disrupted the DHEA-androsterone correlation at M3 (Supplemental figure 2B), which was partially restored at M6 (Supplemental figure 3B). In addition, there was a positive correlation between androsterone sulfate and 2-methyl-3-ketovaleric acid and 2-hydroxy-3-methylbutyric acid as well as 3-formyl-indole. 3-formyl-indole is known as Indole-3-carboxaldehyde (I3A) or indole-3-aldehyde and is a metabolite of dietary L-tryptophan that is synthesized by the gut microbiome. There was a strong correlation with 3-formyl-indole and androsterone levels at both M3 ($p=0.011$) and M6 ($p<0.001$) in the control arm (Fig 5C). This relationship disappeared in the LCD arm at M3 and resumed slightly at M6 (Fig 5D). Therefore, LCD disrupted the correlative relationship between androsterone sulfate with many metabolites at M3, which were partially restored at M6. In contrast, the metabolites which were negatively correlated with the androsterone sulfate in LCD at M6 were only seen in the LCD arm, not in the control arm. Together, these data indicate that LCD at M3 disrupted many correlations between ADT-affected androsterone with glucose, DHEA, 3-formyl-indole seen at both M3 and M6 in the control arms. However, these correlations were partially restored at M6 in LCD arms, suggesting metabolic adaptations.

Discussion

In this study, we applied MS-based metabolomic profiling to determine the effects of LCD intervention after 3 and 6 months of ADT on the serum metabolome of PC participants relative to control patients making no dietary or exercise changes. The key metabolic changes we previously observed as a result of ADT alone (i.e. without diet change) can be summarized into four areas: 1) steroid metabolism, 2) ketogenesis, 3) fatty acid metabolism, and 4) microbiome-associated metabolites. Our current analyses showed that LCD slightly

enhanced the effect of ADT to reduce androgens without reaching statistical significance. LCD intervention also reversed ADT-reduced ketogenesis and acyl-carnitines. LCD also disrupted the correlation between high serum glucose and lower androsterone sulfate and reversed the ADT-induced changes in glycolysis and amino acid metabolisms. Together, LCD intervention significantly reversed many of the ADT-impacted metabolic changes in serum. These data provide mechanistic support for our prior findings that the LCD may mitigate the metabolic side effects of ADT, such as weight gain, worsening insulin resistance, increased hemoglobin A1c, increased HDL, and increased triglycerides as previously reported in the CAPS1 main result paper[10].

To the best of our knowledge, this is the first study to employ serum metabolomics to investigate the effects of LCD in the context of ADT treatment among PC patients. Several previous studies have investigated the metabolic response to LCD in the contexts of other cancers. For example, LCD in people with pancreatic cancer increased serum β-hydroxybutyrate and total ketone levels as well as the glycerophospholipid and sphingolipid metabolisms [38]. In a mouse xenograft study, the progression of breast cancer lead to serum metabolic changes, which were reversed with LCD. LCD also affected the amino acid metabolism and fatty acid transport, suggesting a tumor-suppressing mechanism of LCD when combined with tumor therapeutics [39].

In the primary paper describing the clinical outcomes of CAPS1 trial, LCD did not significantly affect PSA [10]. However, in a follow-up randomized CAPS2 trial, LCD slowed PSA doubling times, when adjusting for baseline differences between the arms [40]. Consistently, while ADT reduced androsterone sulfate in both arms, the reduction showed a tendency to be even more pronounced in the LCD arm. Future research with more participants is warranted to determine whether LCD may enhance the ADT-reduced androsterone sulfate or not. Moreover, given that lower nadir androgen values on ADT are associated with reduced risk of progression [41], this raises the possibility that LCDs may enhance the anti-PC effects of ADT, though this requires formal testing in future studies.

It is also interesting to note the ADT-induced succinyl-adenosine, a metabolite known to accumulate in patients of adenylosuccinate lyase deficiency[37]. Interestingly, patients with adenylosuccinate lyase deficiency exhibit severe neurological impairment ranging from early-onset neonatal epileptic encephalopathy to progressive psychomotor retardation and autism including intellectual disability[42,43]. Recently, ADT has been found to be positively associated with dementia, though whether ADT *causes* dementia or is merely associated with dementia is unclear.[44] Our intriguing correlation suggest a potential mechanistic link between ADT and impaired cognition via elevated succinyl-adenosine. Moreover, the fact that the ADT-increased succinyl-adenosine was abolished by LCD leads to the provocative hypothesis that LCDs may prevent the cognitive decline from ADT. Again, this remains highly speculative and requires further validation in larger studies.

In CAPS1, ketone bodies and acyl-carnitines were shown to be decreased by ADT in the control arm [21]. Ketone bodies are also postulated to affect insulin resistance and increased ketone bodies during ketogenic diets may account for the reduced insulin resistance [45]. Therefore, ADT-associated reduced ketone bodies may contribute to ADT-induced insulin

resistance and justify the potential of ketogenic LCD to reverse these effects. As expected, we noted that LCD increased 3-hydroxybutyric acid at both time points compared to baseline (Fig 2, 3). These results suggest that LCD intervention was effective in overcoming ADT's impact in reducing this metabolite, maybe through the activation of fatty acid β-oxidation and ketogenesis. The increase of 3-hydroxybutyric acid was less dramatic at M6 compared to M3, which may be due to a possible metabolic adaptation or lower adherence to the LCD. However, since the carbohydrate intake and adherence to the LCD were similar at M3 (carb intake: 74.4 gm) and M6 (78.9 gm) vs. BL (227.2 gm) [10], metabolic adaptation may be more likely. High levels of acyl-carnitines were found in diet-induced obesity and insulin resistance in human and mouse models[46,47] and postulated to contribute to insulin resistance phenotypes[48] of ADT. We found that LCD reversed the ADT-reduced acyl-carnitines and the increased acyl-carnitines were strongly clustered with increased ketone-related metabolites[49,50]. Together, these findings suggest a metabolic connection between ketogenesis and altered acyl-carnitines, indicating the ability of LCD to reverse these ADT-induced metabolic changes.

Previously, we found that the degree of ADT-induced androsterone sulfate was strongly associated with the changes in indole-3-carboxaldehyde (ICA), a microbiota-derived metabolite that stimulates aryl hydrocarbon receptors in intestinal immune cells that produce IL-22 [22]. ICA treatments in mice reduced gut inflammation, limited epithelial damage and reduced transepithelial bacterial translocation, and decreased inflammatory cytokines [51]. The disruption of the ADT-ICA in the LCD arm further highlights the metabolic impact of LCD intervention on the chemical exchange between host and microbiome [52]. The increased ketone bodies in ketogenic diets reproducibly inhibited bifidobacterial growth and reduced intestinal pro-inflammatory Th17 cells [52]. These temporary effects indicate that many of the diet-induced changes in the microbiomes may be compensated by the hosts' adaptive response. Therefore, it will be important to identify the nature and mechanisms of these metabolic adaptation to sustain the metabolic effects and therapeutic benefits of LCD.

Our results should be interpreted within the limitations of our study. A small sample size of the cohort may limit our power to detect subtle differences that may be of importance. As such, our results should be considered hypothesis-generating and require validation in larger datasets. Furthermore, it is not clear whether there may be differences in the metabolic response for patients with different tumor grades. In addition, the relative contribution of LCD itself and the walking recommendation to the observed effects cannot be distinguished in this study and needs to be further dissected. Finally, future studies are needed to correlate these metabolomic changes with the long-term outcomes including tumor control and metabolic side effects of ADT such as diabetes risk.

Conclusion

Our findings indicate the metabolic basis for the potential of LCDs in reversing many of the side effects of ADT. However, some of the reversed effects appeared temporary as they were less pronounced at 6-month than at 3-month. Future studies are needed to understand how the effects can be sustained. Further, our study suggests that LCDs may enhance the effect of

ADT by reducing androsterone sulfate and other metabolic mechanisms, though future research is needed to confirm this finding and understand the underlying mechanisms.

Supplementary Material

Refer to Web version on PubMed Central for supplementary material.

Funding and Acknowledgement:

American Urological Association Foundation, BERG, NIH, and Robert C. and Veronica Atkins Foundation

References

1. Siegel RL, Miller KD, Jemal A. Cancer statistics, 2018. CA Cancer J Clin. 2018;68(1):7–30. [PubMed: 29313949]
2. Society AC. Key statistics for prostate cancer. [Webpage]. 2019; https://www.cancer.org/cancer/prostate-cancer/about/key-statistics.html#references. Accessed Febuary 26, 2019.
3. Sweeney CJ, Chen YH, Carducci M, et al. Chemohormonal Therapy in Metastatic Hormone-Sensitive Prostate Cancer. N Engl J Med. 2015;373(8):737–746. [PubMed: 26244877]
4. Fizazi K, Tran N, Fein L, et al. Abiraterone plus Prednisone in Metastatic, Castration-Sensitive Prostate Cancer. N Engl J Med. 2017;377(4):352–360. [PubMed: 28578607]
5. Leong DP, Fradet V, Shayegan B, et al. Cardiovascular Risk in Men with Prostate Cancer: Insights from the RADICAL PC Study. J Urol. 2020:101097JU0000000000000714.
6. Westman EC, Mavropoulos J, Yancy WS, Volek JS. A review of low-carbohydrate ketogenic diets. Curr Atheroscler Rep. 2003;5(6):476–483. [PubMed: 14525681]
7. Yancy WS Jr., Olsen MK, Guyton JR, Bakst RP, Westman EC. A low-carbohydrate, ketogenic diet versus a low-fat diet to treat obesity and hyperlipidemia: a randomized, controlled trial. Ann Intern Med. 2004;140(10):769–777. [PubMed: 15148063]
8. Kossoff EH. More fat and fewer seizures: dietary therapies for epilepsy. Lancet Neurol. 2004;3(7):415–420. [PubMed: 15207798]
9. Hallberg SJ, McKenzie AL, Williams PT, et al. Effectiveness and Safety of a Novel Care Model for the Management of Type 2 Diabetes at 1 Year: An Open-Label, Non-Randomized, Controlled Study. Diabetes Ther 2018;9(2):583–612. [PubMed: 29417495]
10. Freedland SJ, Howard L, Allen J, et al. A lifestyle intervention of weight loss via a low-carbohydrate diet plus walking to reduce metabolic disturbances caused by androgen deprivation therapy among prostate cancer patients: carbohydrate and prostate study 1 (CAPS1) randomized controlled trial. Prostate Cancer and Prostatic Diseases. 2019;22(3):428–437. [PubMed: 30664736]
11. Tang X, Lin CC, Spasojevic I, Iversen E, Chi JT, Marks JR. A joint analysis of metabolomics and genetics of breast cancer Breast Cancer Res. 2014;16(4):415. [PubMed: 25091696]
12. Hakimi AA, Reznik E, Lee CH, et al. An Integrated Metabolic Atlas of Clear Cell Renal Cell Carcinoma. Cancer Cell. 2016;29(1):104–116. [PubMed: 26766592]
13. Vandergrift LA, Decelle EA, Kurth J, et al. Metabolomic Prediction of Human Prostate Cancer Aggressiveness: Magnetic Resonance Spectroscopy of Histologically Benign Tissue. Sci Rep. 2018;8(1):4997. [PubMed: 29581441]
14. Cheng LL, Burns MA, Taylor JL, et al. Metabolic characterization of human prostate cancer with tissue magnetic resonance spectroscopy. Cancer Res. 2005;65(8):3030–3034. [PubMed: 15833828]
15. Sreekumar A, Poisson LM, Rajendiran TM, et al. Metabolomic profiles delineate potential role for sarcosine in prostate cancer progression. Nature. 2009;457(7231):910–914. [PubMed: 19212411]
16. Wang Y, Jacobs EJ, Carter BD, Gapstur SM, Stevens VL. Plasma Metabolomic Profiles and Risk of Advanced and Fatal Prostate Cancer. Eur Urol Oncol. 2019.

17. Gao B, Lue HW, Podolak J, et al. Multi-Omics Analyses Detail Metabolic Reprogramming in Lipids, Carnitines, and Use of Glycolytic Intermediates between Prostate Small Cell Neuroendocrine Carcinoma and Prostate Adenocarcinoma. Metabolites. 2019;9(5).
18. Schmidt JA, Fensom GK, Rinaldi S, et al. Patterns in metabolite profile are associated with risk of more aggressive prostate cancer: A prospective study of 3,057 matched case-control sets from EPIC. Int J Cancer. 2019.
19. Huang G, Liu X, Jiao L, et al. Metabolomic evaluation of the response to endocrine therapy in patients with prostate cancer. Eur J Pharmacol. 2014;729:132–137. [PubMed: 24556387]
20. Saylor PJ, Karoly ED, Smith MR. Prospective study of changes in the metabolomic profiles of men during their first three months of androgen deprivation therapy for prostate cancer. Clin Cancer Res. 2012;18(13):3677–3685. [PubMed: 22589396]
21. Chi JT, Lin PH, Tolstikov V, et al. Metabolomic effects of androgen deprivation therapy treatment for prostate cancer. Cancer Med. 2020.
22. Zelante T, Iannitti RG, Cunha C, et al. Tryptophan catabolites from microbiota engage aryl hydrocarbon receptor and balance mucosal reactivity via interleukin-22. Immunity. 2013;39(2):372–385. [PubMed: 23973224]
23. Gacias M, Gaspari S, Santos PM, et al. Microbiota-driven transcriptional changes in prefrontal cortex override genetic differences in social behavior. Elife. 2016;5.
24. Bajad S, Shulaev V. LC-MS-based metabolomics. Methods Mol Biol. 2011;708:213–228. [PubMed: 21207293]
25. Kiebish MA, Cullen J, Mishra P, et al. Multi-omic serum biomarkers for prognosis of disease progression in prostate cancer. J Transl Med 2020;18(1):10. [PubMed: 31910880]
26. Tolstikov V, Nikolayev A, Dong S, Zhao G, Kuo MS. Metabolomics analysis of metabolic effects of nicotinamide phosphoribosyltransferase (NAMPT) inhibition on human cancer cells. PLoS One. 2014;9(12):e114019. [PubMed: 25486521]
27. Dunn WB, Broadhurst D, Begley P, et al. Procedures for large-scale metabolic profiling of serum and plasma using gas chromatography and liquid chromatography coupled to mass spectrometry. Nat Protoc 2011;6(7):1060–1083. [PubMed: 21720319]
28. Xia J, Wishart DS. MSEA: a web-based tool to identify biologically meaningful patterns in quantitative metabolomic data. Nucleic Acids Res. 2010;38(Web Server issue):W71–77. [PubMed: 20457745]
29. Tang X, Wu J, Ding CK, et al. Cystine Deprivation Triggers Programmed Necrosis in VHL-Deficient Renal Cell Carcinomas. Cancer Res. 2016;76(7):1892–1903. [PubMed: 26833124]
30. Tang X, Ding CK, Wu J, et al. Cystine addiction of triple-negative breast cancer associated with EMT augmented death signaling. Oncogene. 2017;36(30):4379. [PubMed: 28604749]
31. Yang W-H, Lin C-C, Wu J, et al. The Hippo Pathway Effector YAP Promotes Ferroptosis via the E3 Ligase SKP2. Molecular Cancer Research. 2021:molcanres.0534.2020.
32. Chen PH, Wu J, Xu Y, et al. Zinc transporter ZIP7 is a novel determinant of ferroptosis. Cell Death & Disease. 2020;In Press.
33. Yamamoto H, Fujimori T, Sato H, Ishikawa G, Kami K, Ohashi Y. Statistical hypothesis testing of factor loading in principal component analysis and its application to metabolite set enrichment analysis. BMC Bioinformatics. 2014;15:51. [PubMed: 24555693]
34. Gatza ML, Kung HN, Blackwell KL, Dewhirst MW, Marks JR, Chi JT. Analysis of tumor environmental response and oncogenic pathway activation identifies distinct basal and luminal features in HER2-related breast tumor subtypes. Breast Cancer Res. 2011;13(3):R62. [PubMed: 21672245]
35. Chen JL, Merl D, Peterson CW, et al. Lactic acidosis triggers starvation response with paradoxical induction of TXNIP through MondoA. PLoS Genet. 2010;6(9).
36. Labadie BW, Bao R, Luke JJ. Reimagining IDO Pathway Inhibition in Cancer Immunotherapy via Downstream Focus on the Tryptophan–Kynurenine–Aryl Hydrocarbon Axis. Clinical Cancer Research. 2019;25(5):1462–1471. [PubMed: 30377198]
37. Jurecka A, Zikanova M, Kmoch S, Tylki-Szymańska A. Adenylosuccinate lyase deficiency. J Inherit Metab Dis. 2015;38(2):231–242. [PubMed: 25112391]

38. Kang CM, Yun B, Kim M, et al. Postoperative serum metabolites of patients on a low carbohydrate ketogenic diet after pancreatectomy for pancreatobiliary cancer: a nontargeted metabolomics pilot study. Scientific Reports. 2019;9(1):16820. [PubMed: 31727967]
39. Licha D, Vidali S, Aminzadeh-Gohari S, et al. Untargeted Metabolomics Reveals Molecular Effects of Ketogenic Diet on Healthy and Tumor Xenograft Mouse Models. Int J Mol Sci. 2019;20(16).
40. Freedland SJ, Allen J, Jarman A, et al. A Randomized Controlled Trial of a 6-Month Low-Carbohydrate Intervention on Disease Progression in Men with Recurrent Prostate Cancer: Carbohydrate and Prostate Study 2 (CAPS2). Clin Cancer Res. 2020;26(12):3035–3043. [PubMed: 32108029]
41. Klotz L, O'Callaghan C, Ding K, et al. Nadir testosterone within first year of androgen-deprivation therapy (ADT) predicts for time to castration-resistant progression: a secondary analysis of the PR-7 trial of intermittent versus continuous ADT. J Clin Oncol. 2015;33(10):1151–1156. [PubMed: 25732157]
42. Banerjee A, Bhatia V, Didwal G, Singh AK, Saini AG. ADSL Deficiency - The Lesser-Known Metabolic Epilepsy in Infancy. Indian J Pediatr. 2020.
43. Macchiaiolo M, Buonuomo PS, Mastrogiorgio G, et al. Very mild isolated intellectual disability caused by adenylosuccinate lyase deficiency: a new phenotype. Mol Genet Metab Rep. 2020;23:100592. [PubMed: 32405461]
44. Cui H, Wang Y, Li F, et al. Quantifying observational evidence for risk of dementia following androgen deprivation therapy for prostate cancer: an updated systematic review and meta-analysis. Prostate Cancer Prostatic Dis. 2020.
45. Veech RL. The therapeutic implications of ketone bodies: the effects of ketone bodies in pathological conditions: ketosis, ketogenic diet, redox states, insulin resistance, and mitochondrial metabolism. Prostaglandins Leukot Essent Fatty Acids. 2004;70(3):309–319. [PubMed: 14769489]
46. Mihalik SJ, Goodpaster BH, Kelley DE, et al. Increased Levels of Plasma Acylcarnitines in Obesity and Type 2 Diabetes and Identification of a Marker of Glucolipotoxicity. Obesity. 2010;18(9):1695–1700. [PubMed: 20111019]
47. Koves TR, Ussher JR, Noland RC, et al. Mitochondrial overload and incomplete fatty acid oxidation contribute to skeletal muscle insulin resistance. Cell Metab. 2008;7(1):45–56. [PubMed: 18177724]
48. Schooneman MG, Vaz FM, Houten SM, Soeters MR. Acylcarnitines. Reflecting or Inflicting Insulin Resistance? 2013;62(1):1–8. [PubMed: 23258903]
49. Dambal S, Alfaqih M, Sanders S, et al. 27-Hydroxycholesterol Impairs Plasma Membrane Lipid Raft Signaling as Evidenced by Inhibition of IL6–JAK–STAT3 Signaling in Prostate Cancer Cells. Molecular Cancer Research. 2020;18(5):671–684. [PubMed: 32019810]
50. Alfaqih MA, Nelson ER, Liu W, et al. CYP27A1 Loss Dysregulates Cholesterol Homeostasis in Prostate Cancer. Cancer Research. 2017;77(7):1662–1673. [PubMed: 28130224]
51. Swimm A, Giver CR, DeFilipp Z, et al. Indoles derived from intestinal microbiota act via type I interferon signaling to limit graft-versus-host disease. Blood. 2018;132(23):2506–2519. [PubMed: 30257880]
52. Ang QY, Alexander M, Newman JC, et al. Ketogenic Diets Alter the Gut Microbiome Resulting in Decreased Intestinal Th17 Cells. Cell. 2020;181(6):1263–1275 e1216. [PubMed: 32437658]

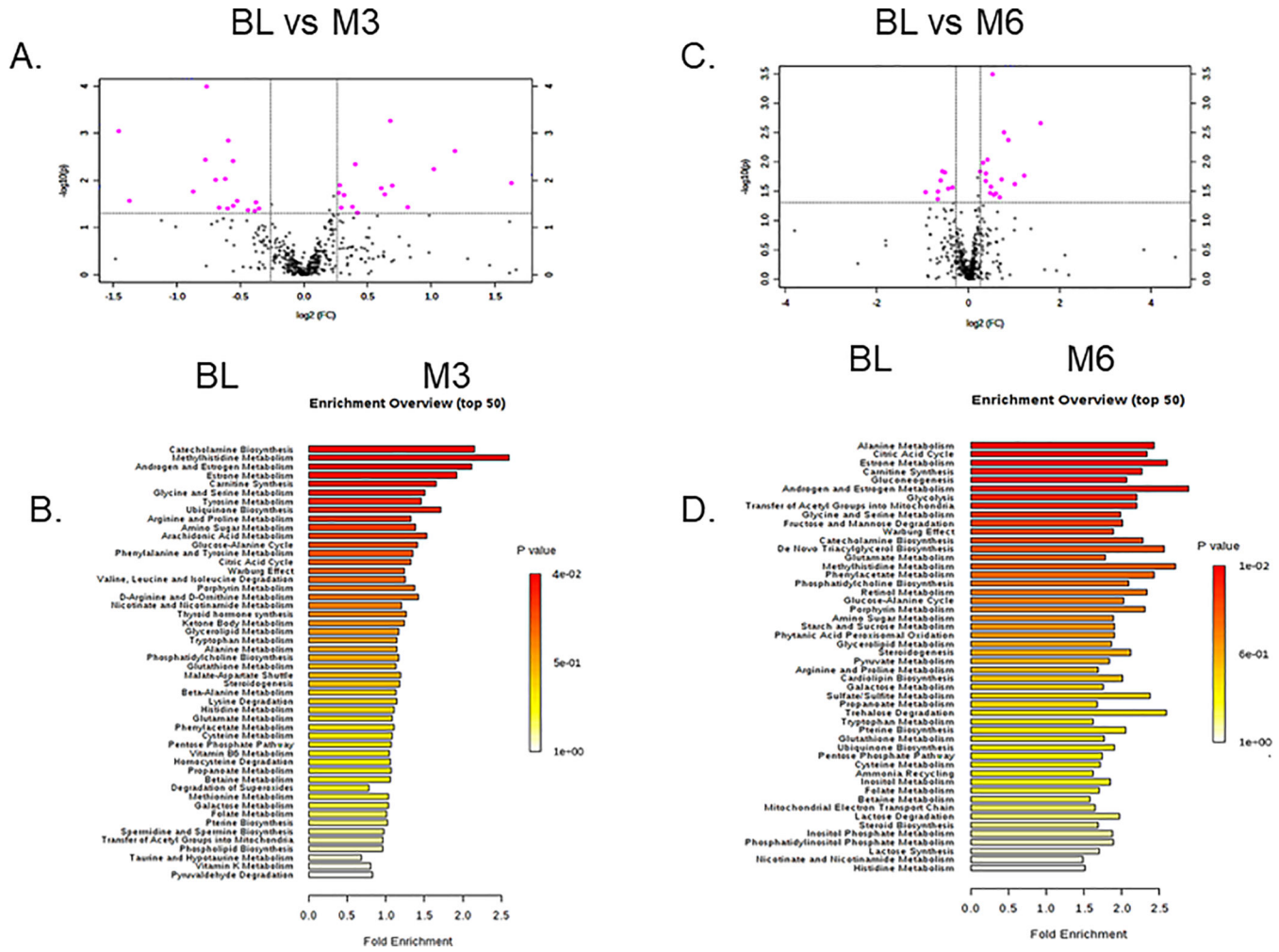

Figure 1: Top serum metabolites and metabolic pathways altered at 3- and 6-month after initiating ADT treatments in participants receiving LCD.

(A) Metabolites were selected by Volcano plot analysis of pairwise comparison between the BL vs. M3 (A) and BL vs. M6 (C) ADT. (B, D) Top enriched metabolic pathways affected by ADT after M3 (B) and M6 (D) of LCD.

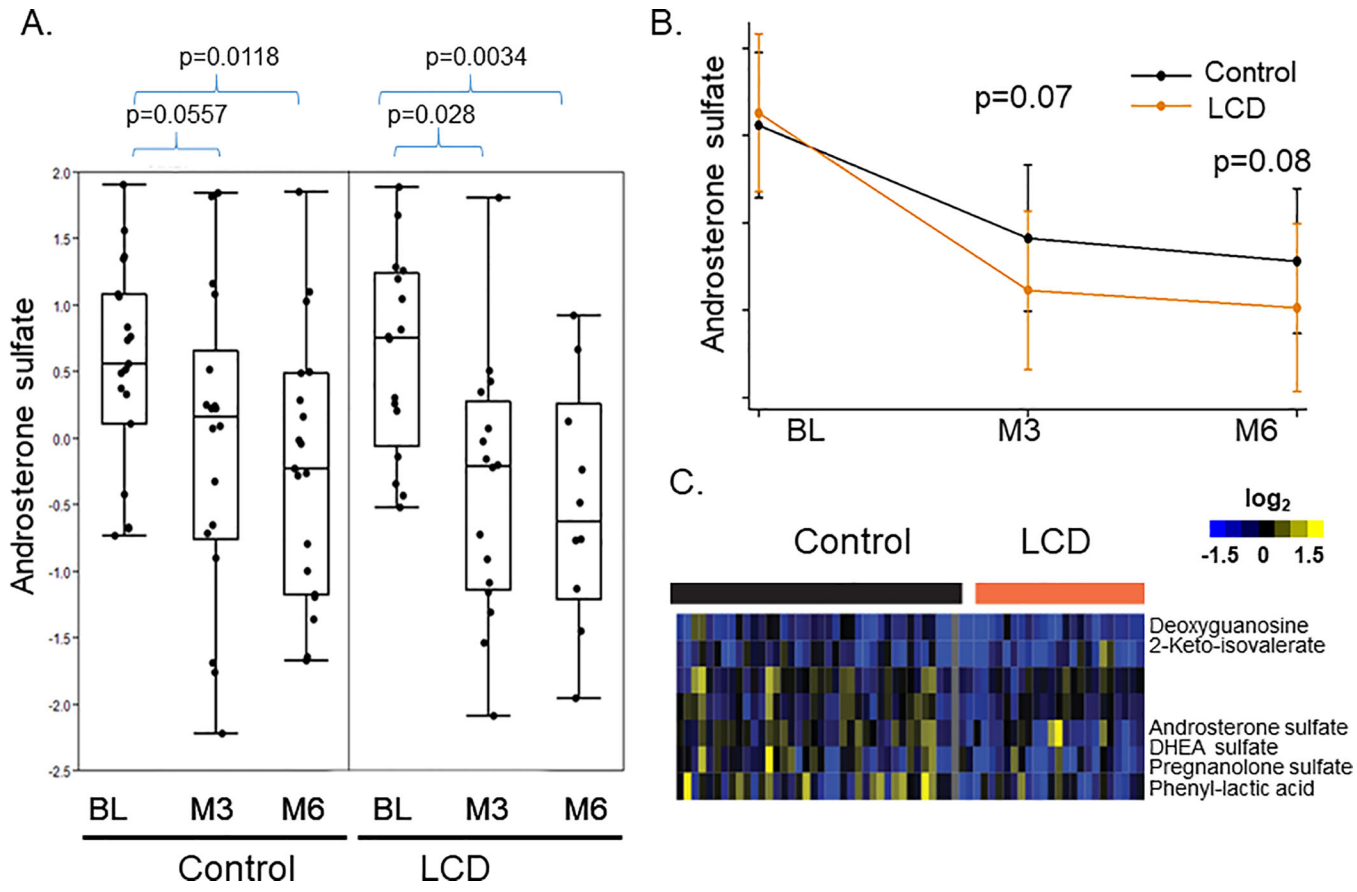

Figure 2: The effects of LCD on the ADT-affected androsterone sulfate and related metabolites

(A) ADT reduced the levels of androsterone sulfate in both control and LCD arms. (B) The mean levels of the androsterone sulfate in the control and LCD arms at the BL, M3 and M6. (C) Heatmap of the clusters of metabolites that were altered in ways similar to androsterone sulfate.

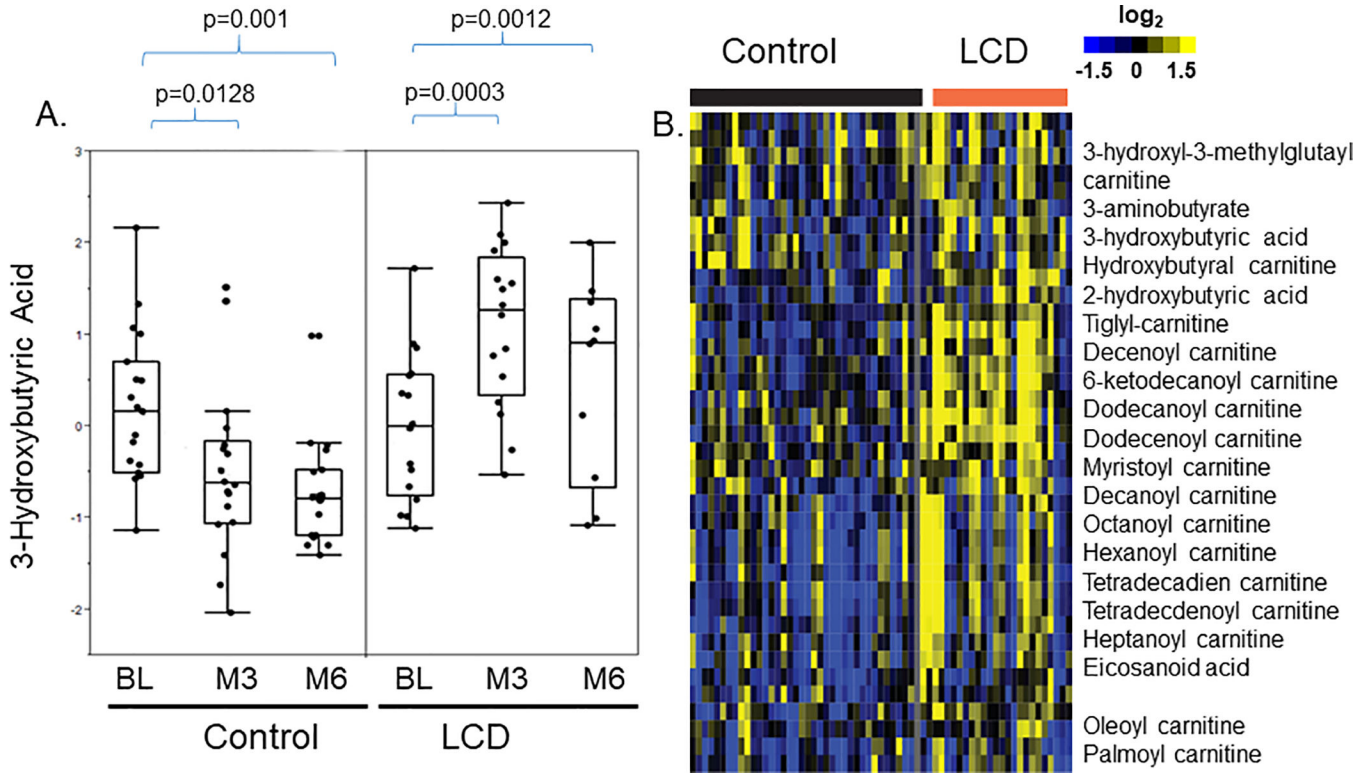

Figure 3: The effects of LCD on the ADT-affected 3-hydroxy-butyric acid

(A) The effects of ADT-induced changes in the 3-hydroxy-butyric acid in the control and LCD arms at M3 and M6. (B) Heatmap of the clusters of metabolites that were altered in ways similar to 3-hydroxy-butyric acid. The statistical significance (p values) of ADT-induced changes of indicated metabolites is indicated.

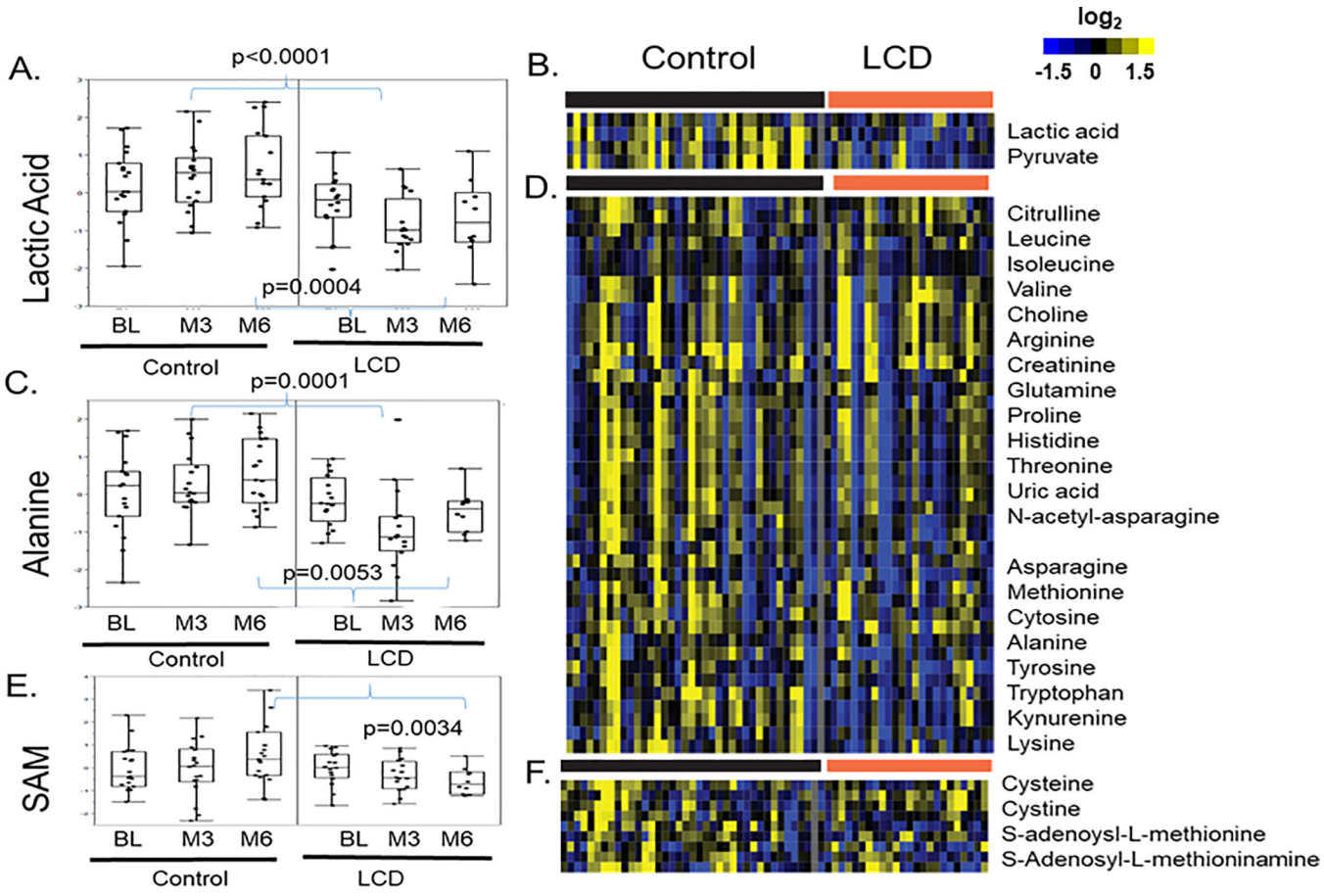

Figure 4: The effects of LCD on the ADT-altered lactic acid, alanine and S-adenosyl-L-methionine (SAM)

(A) The effects of ADT-induced changes in the lactic acid in the control and LCD arms at M3 and M6. (B) Heatmap of the clusters of metabolites that were altered in ways similar to lactic acid. (C) The effects of ADT-induced changes in the alanine in the control and LCD arms at M3 and M6. (D) Heatmap of the clusters of metabolites that were altered in ways similar to alanine. (E) The effects of ADT-induced changes in the S-adenosyl-L-methionine (SAM) in the control and LCD arms at M3 and M6. (F) Heatmap of the clusters of metabolites that were altered in ways similar to SAM. The statistical significance (p values) of ADT-induced changes of indicated metabolites is indicated.

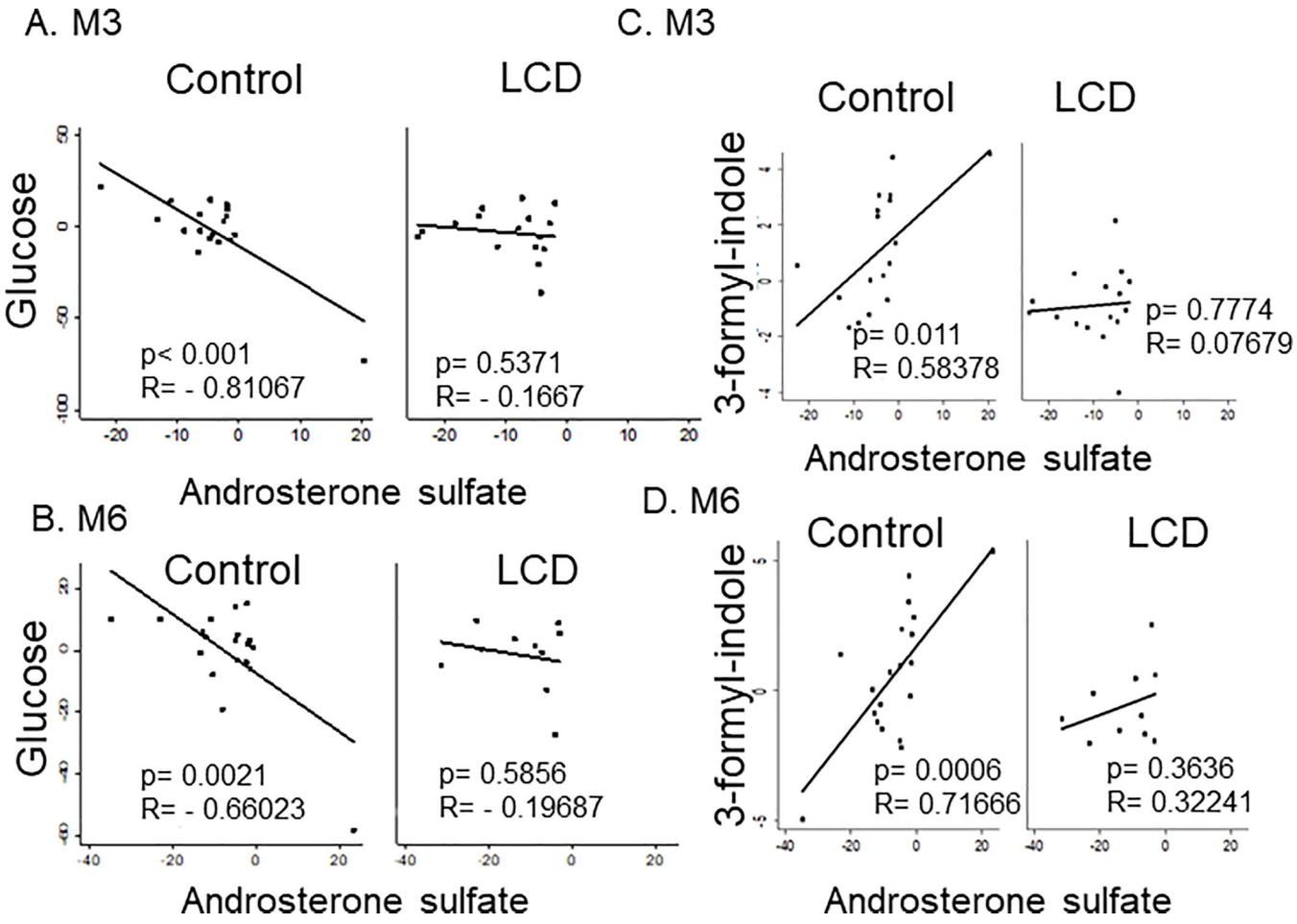

Figure 5: Serum chemistry and metabolites correlated with ADT-reduced androsterone sulfate

(A-B) The correlation between the ADT-induced changes in the androsterone sulfate and serum glucose in the control and LCD arm after 3 (A) and 6 months (B) of ADT. (C, D) The correlation plots between the ADT-induced changes in the 3-formyl-indole with androsterone sulfate at M3 (C) and M6 (D) in the control and LCD arms.